Electronic Sculpting of Ligand-GPCR Subtype Selectivity: The Case of Angiotensin II

Francesca Magnani,[†,○] Charalampos G. Pappas,[‡] Tim Crook,[§] Vassiliki Magafa,[∥] Paul Cordopatis,[∥] Susumu Ishiguro,[⊥] Naomi Ohta,[⊥] Jana Selent,[¶] Sanja Bosnyak,[#] Emma S. Jones,[#] Ioannis P. Gerothanassis,[‡] Masaaki Tamura,[§] Robert E. Widdop,[#] and Andreas G. Tzakos*[‡,△]

[†]Laboratory of Molecular Biology, Medical Research Council, Cambridge CB2 0QH, United Kingdom

[‡]Department of Chemistry, University of Ioannina, Ioannina 45110, Greece

[§]Division of Cancer Research, University of Dundee, Dundee DD1 9SY, United Kingdom

[∥]Department of Pharmacy, University of Patras, Patra 26504, Greece

[⊥]Department of Anatomy & Physiology, Kansas State University College of Veterinary Medicine, Manhattan, Kansas 66506, United States

[¶]Research Programme on Biomedical Informatics (GRIB), Department of Experimental and Health Sciences, Universitat Pompeu Fabra, IMIM (Hospital del Mar Medical Research Institute), Dr. Aiguader 88, E-08003 Barcelona, Spain

[#]Department of Pharmacology, Monash University, Clayton, Victoria 3800, Australia

[△]Cancer Biobank Center, University of Ioannina, Ioannina 45110, Greece

S *Supporting Information*

ABSTRACT: GPCR subtypes possess distinct functional and pharmacological profiles, and thus development of subtype-selective ligands has immense therapeutic potential. This is especially the case for the angiotensin receptor subtypes AT1R and AT2R, where a functional negative control has been described and AT2R activation highlighted as an important cancer drug target. We describe a strategy to fine-tune ligand selectivity for the AT2R/AT1R subtypes through electronic control of ligand aromatic-prolyl interactions. Through this strategy an AT2R high affinity (K_i = 3 nM) agonist analogue that exerted 18,000-fold higher selectivity for AT2R versus AT1R was obtained. We show that this compound is a negative regulator of AT1R signaling since it is able to inhibit MCF-7 breast carcinoma cellular proliferation in the low nanomolar range.
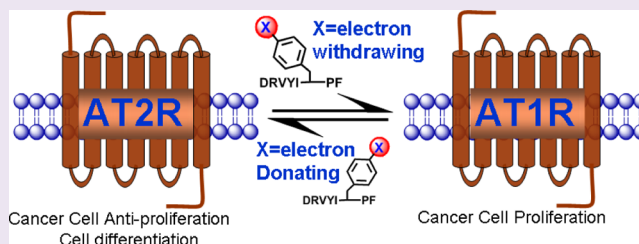
G-protein-coupled receptors (GPCRs) orchestrate most cellular responses to neurotransmitters and hormones.[1] They form a major therapeutic platform for an array of diseases, with 50% of clinically marketed drugs targeting this receptor family.[2] GPCR subtypes within a subfamily usually possess distinct functional and pharmacological profiles,[3] and thus development of subtype-selective ligands has immense untapped therapeutic potential. This is clearly evident for two of the Angiotensin II (AII) receptor subtypes, AT1R and AT2R. Although they are recognized with similar affinity by the hormone AII (NH2-DRVYIHPF-OH),[4,5] the effects of AT2R activation (vasodilation, apoptosis, and antiproliferation) antagonize those mediated by AT1R (cellular growth and proliferation for AT1).[6,7] Since AT2R stimulation has been implicated in tumor suppression,[8,9] tissue repair and regeneration, this receptor has been assigned as an important pharmaceutical drug target.[8,10−13] Therefore, a fine-tuning of the different functional responses of AT1R and AT2R by the use of receptor subtype-selective ligands could be a powerful therapeutic tool.[12]

However, significant challenges are posed for the rational design of GPCR subtype-selective ligands due to the high sequence conservation within the receptor subfamily.[3] Indeed, in the absence of detailed knowledge of ligand−receptor recognition interactions for AT2R, identification of AT2R-selective ligands came after long and delicate synthetic efforts.[10,14] Here, we describe a strategy to fine-tune ligand selectivity for the AT2R/AT1R subtypes through electronic control of ligand aromatic-prolyl interactions (Figure 1). On the basis of this strategy, a highly AT2R-selective (18,000-fold higher selectivity (IC50AT1R/IC50AT2R)) and high affinity agonist analogue (K_i = 3 nM) that exerted antiproliferative activity against MCF-7 breast carcinoma cells was obtained, pointing to a rational way to generate highly receptor subtype-selective drugs.
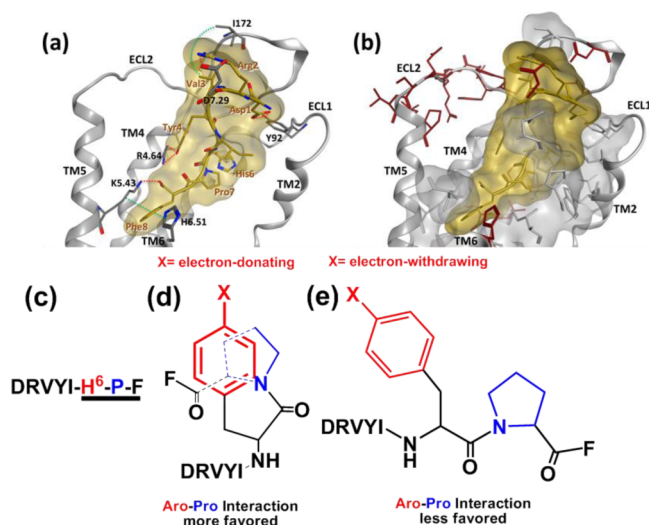
Figure 1. 3D model of the AII−AT1R complex and the electronic tuning strategy used in this work for AII. (a) Key interactions between the hormone AII (yellow stick and surface) and AT1R (gray stick), comprising hydrogen bonds (red dashed line) and hydrophobic contacts (green dashed line). (b) Conserved regions between AT1R and AT2R depicted in gray stick and surface; unconserved regions are highlighted in a red stick representation. ECL1, ECL2 correspond to the extracellular loops 1 and 2 and TM2, 4, 5, and 6 correspond to transmembrane regions 2, 4, 5, and 6, respectively. (c) The sequence of the hormone AII with its C-terminus highlighted. (d,e) The H^6 of AII was altered in this work with 4-X substituted phenylalanine on the frame of an electronic strategy to regulate the compactness of the AII C-terminus. In (d) electron-rich aromatic residues stabilize the aromatic-prolyl interactions and lead to compactness,[18] and in (e) electron-deficient aromatic residues result in less favorable aromatic-prolyl interactions and relatively reduced compactness.

Engineering the Hormone AII To Be Selective for AT2R. Recent exciting advances in the field of GPCR structural biology have provided unprecedented insights into the GPCR fold and the ligand binding pocket architecture.[1] This knowledge has allowed the generation of models for the AT1R bound to AII.[15−17] AII binds to the two receptors with similar affinity (K_{dAT1R} = 1.8 nM, K_{dAT2R} = 2.3 nM; Supplementary Table S3). To guide the design of subtype-selective ligands for AT2R/AT1R, we constructed the receptor models bound to AII and screened for potential hotspot areas that could be discriminative between the two receptor subtypes (Figure 1). AT2R and AT1R are characterized by a sequence identity of 36.5% and similarity of 56.7% (see also full sequence alignment, Supplementary Figure S1). Even higher identity (40.4%) and similarity (60.1%) are observed in the trans-membrane region, where a large portion of the ligand binds. Although in our model AII was embedded in a receptor area with high conservation in both receptors (gray stick and surface, Figure 1b), a diverse region was located at the extracellular loop 2 (ECL2) (red stick, Figure 1b) and the orthosteric pocket (top of TM5 and middle of TM6) that could serve as a ligand-receptor subtype selectivity region. At this point, one has to bear in mind that the ECL2 is a very flexible region and therefore challenging to model. From our model and in accordance with literature data,[15,16] it was pinpointed that the C-terminus of AII, which carries a Pro at position 7 followed by Phe (Figure 1c,b), penetrates deeper into the receptor ligand binding site.

Exploring these unconserved receptor regions revealed the presence of more hydrophobic and larger residues that limit the binding pocket of AT2R relative to AT1R in our obtained structural models (VAT2R 1694 Å^3 < VAT1R 1825 Å^3; for calculation see Supporting Information). It could thus follow that a more hydrophobic and compact motif that exploits this receptor region should be sought for an analogue to be selective for AT2R. Similar observations on the ligand-receptor subtype selectivity were highlighted for other GPCR families such as the nociceptin δ-OR receptors: although presenting high residue conservation on their ligand binding site, ligand selectivity for those receptors was based on a few critical alterations of smaller to larger residues.[19] However, ligand selectivity for β-adrenergic receptor (AR) subtypes was assigned to polar residue alteration.[20]

We postulated that an electronic strategy[18,21] could be adopted in the C-terminus of AII, where Pro^7 is located, to control and tune the compactness of the C-terminus of AII analogues and thus their receptor subtype selectivity (Figure 1c−e). According to this strategy, an aromatic-prolyl interaction can be stabilized by a C−H/π interaction, where the aromatic ring donates electron density (π-electron donor) to the electron-deficient C−H bonds of the pyrrolidine ring.[18] Therefore, electron-rich aromatic residues, shaped after appropriate positioning of an electron-donating group (such as -OH) at the 4-X position of an aromatic ring, preceding a proline, should have the potential to stabilize the aromatic-prolyl interaction (Figure 1d). Thus, this interaction should lead to a more compact conformation for the specific residues and high selectivity for the AT2R. In contrast, electron-deficient aromatic residues, created after installing an electron-with-drawing group (i.e., NO$_2$) at the 4-X position of an aromatic ring, followed by a proline, should lead to less favorable interactions and thus lower compactness and lower selectivity for AT2R (Figure 1e). Thus, we hypothesized that appropriate manipulation/tuning of the electronics of an aromatic ring (position 6 of AII) adjacent to a proline ring (position 7 of AII) could result in a delicate electronic control/tuning of C−H/π interactions and thus regulation of GPCR-ligand subtype selectivity.

To test the validity of this hypothesis, we synthesized AII analogues, substituting the His at position 6 of the AII with 4-substituted phenylalanine with electron-rich (-OH), electron-neutral (-H and -OPO$_3$H$_2$), and electron-deficient (-NO$_2$) groups. To monitor the compactness of the synthesized molecules, we used as an internal sensor the NMR derived % cis character of the Aro^6−Pro^7 amide bond, since it has been established that the strength of the aro-pro compactness follows a positive correlation with the cis isomerization state of the aromatic-prolyl amide bond.[18] The 4-NO$_2$-phenylalanine AII analogue, an electron-deficient aromatic residue (Hammett substituent constant σ_{para} = 0.78), should mostly disfavor the aro-pro interaction and present a minor cis conformation, whereas phenylalanine and phospho-tyrosine ($\sigma_{para} \approx 0.00$ and 0.26, respectively) should generate moderate compactness and cis conformation. Finally, tyrosine, an electron-rich aromatic residue ($\sigma_{para} \approx -0.37$), should favor aro-pro compactness. Supporting this hypothesis, our NMR data indicated that electron-rich residues favored the aromatic-prolyl interaction and the cis amide bonds, with the following ranking order of aromatic substituents: −-OH > -H ≈ -OPO$_3$H$_2$ > -NO$_2$ (the % cis was found to be 40%, 20%, 25%, and 5%, respectively).

[Y]⁶-AII Shows Enhanced *cis* Isomerization and Aromatic-Prolyl Compactness in Solution. To further probe the [Y]⁶-AII analogue structure in solution we used NMR. A selected region of the ¹H−¹H 2D NOESY spectrum of the analogue is shown in Figure 2. Interestingly, in aqueous
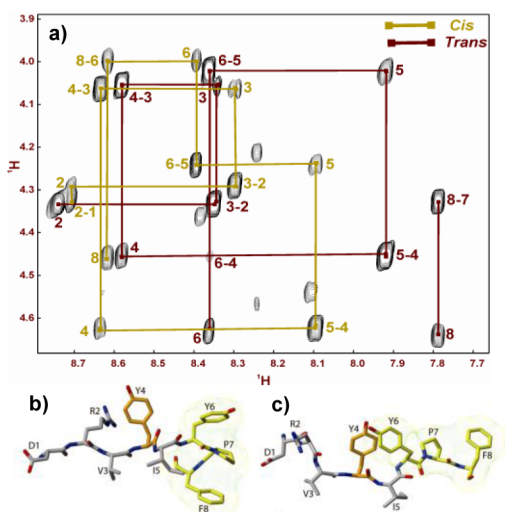

Figure 2. (a) Selected region of a 350 ms NOESY spectrum of [Y]⁶-AII (90% H_2O/10% D_2O). The red and green lines denote the NOE connectivities for the *trans* and *cis* isomers, respectively. Solution structures of the distinctive *cis* (b) and *trans* (c) conformers of the engineered AII analogue.

solution [Y]⁶-AII showed two distinct sets of proton resonances that correspond to discrete *cis* and *trans* conformational populations. This was in contrast to the native AII where a single set of peaks was observed, representing the single conformer (*trans*) (Supplementary Figure S2−S4). This structural plasticity (coexistence of nearly equal populations in solution of two different discrete conformations) could be favorable for recognition selectivity. Due to excellent dispersion of the resonances of the *cis* and *trans* conformers, deconvolution and complete resonance assignment was achieved (Supplementary Tables S1 and S2). Structure calculations for the distinctive *cis* and *trans* isomers were performed, and the structural origin of the stabilization of the relevant conformational potencies was mapped (Figure 2). As was expected, for the [Y]⁶-AII *cis* isomer the calculations produced a family of structures with the aromatic rings of Tyr⁶ and Phe⁸ stacked around the Pro⁷ ring, thus leading to a compact hydrophobic motif (Figure 2b). The structural architecture of this motif was found to mimic closely the conformation adopted by Tyr-Pro-Phe minicores recorded in the crystallographic protein database (Supplementary Figure S5). The compactness of the *cis* over the *trans* form was also probed through a more reduced accessibility of the peptide bonds as determined from both the amide proton temperature coefficients and translational diffusion values (i.e., for Tyr⁴ we determined a diffusion coefficient of 1.9×10^{-10} m² s⁻¹ for the *cis* and 2.3×10^{-10} m² s⁻¹ for the *trans*, Supplementary Figure S6).

[Y]⁶-AII Analogue Is Selective for AT2R. Since the [Y]⁶-AII analogue experimentally fulfilled the selectivity criteria for AT2R hypothesized at the onset of this study, we measured its binding to AT1R and AT2R recombinantly expressed in mammalian cells. Interestingly, the analogue ligated AT2R with

high affinity (K_i = 3.4 ± 0.8 nM), whereas saturable binding to AT1R was in the submillimolar range (Supplementary Table S3). In order to elucidate whether the [Y]⁶-AII AT2R subtype selectivity was due to the effectiveness of the electronic tuning of the aromatic-prolyl interaction, we then performed binding experiments of the rest of the analogues to the AT1R and AT2R (Figure 3, Supplementary Tables S4 and S5). Notably,
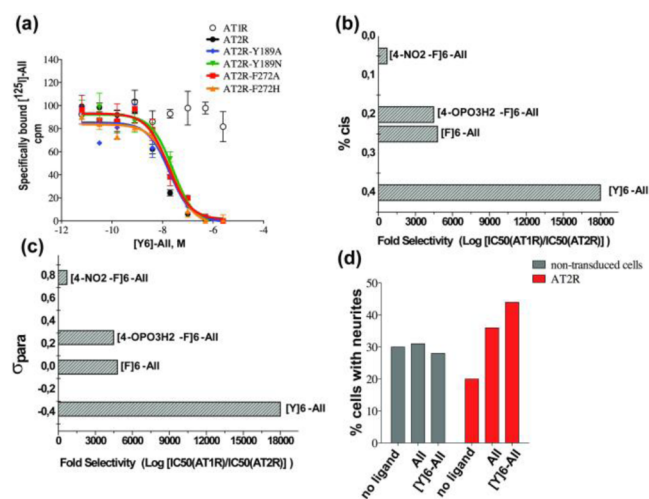

Figure 3. (a) Competition binding assays of [Y]⁶-AII analogue to AT1R, AT2R wild type, and mutants: AT1R, open circle; wild type AT2R, black circles; AT2R-Y189A, blue diamonds; AT2R-Y189N, green triangle; AT2R-F272(6.51)A, red square; AT2R-F272(6.51)H, orange triangle. K_d and K_i values are given in Supplementary Table S3. (b,c) Plots of fold selectivity values for the two AII receptor subtypes (IC_{50}(AT1R)/IC_{50}(AT2R)]) versus % of *cis* (b) and the value of Hammet substituent constants σ_{para} (c) for the different AII analogues (see also Supplementary Table S5). (d) PC12W cells, either transduced with the Ad-AT2R or untransduced, were used for the evaluation of the AT2R agonistic effect of [Y]⁶-AII in the presence of either 1 nM AII or [Y]⁶-AII. Agonist-induced neurite outgrowth by AII or [Y]⁶-AII for 24 h stimulation was quantified by counting neurite-positive cell numbers in five randomly selected photos/well. The neurite outgrowth-positive cells were defined as the cells with neurite length longer than their cell diameters. This experiment was carried out in triplicate and repeated twice.

the AT2R/AT1R fold selectivity of all the AII analogues was directly correlated to the aro-pro compactness of the analogues as described above (Figure 3, Supplementary Table S5): the [Y]⁶-AII analogue presented a 18,000-fold higher selectivity (IC_{50}AT1R/IC_{50}AT2R); [4-OPO₃H₂-F]⁶-AII and [F]⁶-AII showed similar receptor subtype selectivities (4479 and 4786, respectively). In contrast and as expected, [4-NO₂-F]⁶-AII presented a much lower (26-fold less) selectivity for the AT2R/AT1R receptor subtypes (694).

Potential Localization of the [Y]⁶-AII Analogue in the AT2 Receptor: Modeling and Functional Data. In order to assess the origin of the highest selectivity of the [Y]⁶-AII analogue to the AT2R over the AT1R, the relevant analogue was docked into the two receptors (Figure 4). Residues that interact with the [Y]⁶-AII analogue in both receptors (Supplementary Figure S7) are also listed in Supplementary Table S6 containing their residue ID as well as the corresponding Ballesteros-Weinstein numbering.[22]

[Y]⁶-AII adopted a more compact and stacked conformation in the Tyr⁶-Pro⁷-Phe⁸ region, as well as a slightly deeper penetration into the binding pocket of AT2R with respect to
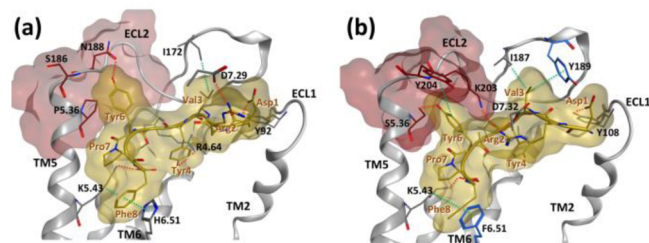
Figure 4. Structure of [Y]⁶-AII in complex with AT1R (a) and AT2R (b). [Y]⁶-AII is shown in yellow stick and surface, and unconserved regions in AT1R and AT2R are shown in red stick and surfaces. Red dashed lines correspond to hydrogen bonds, and green dashed lines to hydrophobic contacts. Residues depicted in blue stick were mutated for validation of the binding mode.

AT1R (see also Supplementary Figure S8). To this contributed unconserved regions between the two receptors that were mainly mapped in TM5 (top region) and the ECL2 region.

On the other hand, unconserved residues in the ECL2 of AT2R (red stick and surface, Figure 4) and in particular the aromatic Y^{189} that contributes to the formation of a hydrophobic groove that favorably accommodated V^3 of [Y]⁶-AII seem to push the analogue deeper in the transmembrane region of the AT2R to develop the favorable F^8 ([Y]⁶-AII)−$F^{272(6.51)}$ (AT2R) stacking interaction (the Ballesteros-Weinstein numbering[22] of F^{272} is shown in parentheses). Y^{189} and $F^{272(6.51)}$ of AT2R, which seem to develop the aforementioned favorable interactions with the N- and C-termini of [Y]⁶-AII, are altered to N^{174} and $H^{256(6.51)}$, respectively, in AT1R. In order to verify that, among others, these residues are also responsible for the [Y]⁶-AII affinity and selectivity to AT2R/AT1R, we made the following AT2R mutants: Y^{189}A, Y^{189}N, $F^{6.51}$A, and $F^{272(6.51)}$H. These changes introduced in AT2R polar residues or residues of smaller size near the ligand binding pocket, thus emulating the environment in the AT1R ligand binding pocket. Both AII and [Y]⁶-AII were used to probe the binding pocket of AT2R and its variants. The affinity of AII, which has histidine at position 6, was not altered for the AT2R mutants with respect to the wild type receptor. It was interesting to note that the affinity of AII was slightly higher for the AT2R mutants emulating the environment in the AT1R (Y^{189}N and $F^{272(6.51)}$H) compared to the Y^{189}A and $F^{272(6.51)}$ AT2R variants (Supplementary Table S3). However, [Y]⁶-AII presented a largely reduced affinity for the AT2R variants by a factor of 4 to 5 folds with respect to the wild type receptor (Supplementary Table S3). Overall, these data support the initial hypothesis that the [Y]⁶-AII superior selectivity to AT2R is based on a more hydrophobic and compact binding pocket (compared to AT1R).

[Y]⁶-AII Analogue Is an AT2R Agonist and a Negative Regulator of AT1R Signaling. To evaluate if the tight binder and subtype AT2R-selective [Y]⁶-AII analogue could serve as a desired AT2R agonist, we monitored its effect on cell differentiation (neurite outgrowth) in AT2R-overexpressing PC12W cells. PC12W cells have been shown to be capable of expressing AT2R in lengthy serum-free culture conditions,[23] and their neurite outgrowth is stimulated by AII.[24] As shown in Figure 3d, both AII and the [Y]⁶-AII analogue significantly stimulated neurite outgrowth in the AT2R transduced cells. This phenotype was ligand dose-dependent in the range of 1 pM to 100 nM for both AII and [Y]⁶-AII.

A functional negative crosstalk among AT2R and AT1R has been extensively described in several pathophysiological conditions including cancer,[25,26] evidencing AT2R activation as an important cancer drug target.[8,9,27] To probe the efficacy of our AT2R-selective [Y]⁶-AII agonist to act as a negative regulator of AT1R signaling, we focused on MCF-7 breast carcinoma cells where both AT1R and AT2R are expressed[28] and native AII stimulates cellular proliferation through AT1R binding.[28] We assessed the effect of [Y]⁶-AII in MCF-7 cell proliferation by growth curves comparing [Y]⁶-AII-treated cells with vehicle-treated control cells (Supplementary Figure S11). As was expected, [Y]⁶-AII efficiently inhibited MCF-7 proliferation at concentrations of 10^{-8} M and showed evidence of antiproliferative effects at 10^{-9} M (IC_{50} of ∼5 × 10^{-8} M).

Here, we demonstrated that AII receptor subtype selectivity could be precisely sculpted by tuning the electronic character of a simple substitution of the hydrogen in the *para*-position of phenylalanine introduced at position 6 of AII (4-x-Phe⁶). Specifically, the [Y]⁶-AII analogue with an electron-donating group (-OH) resulted in a selective and high affinity binder for AT2R (K_i = 3.4 ± 0.8 nM), whereas electron-withdrawing groups diminished high selectivity for this receptor subtype. Most importantly, this receptor recognition phenotype is directly correlated to the compactness of the 4-X-Phe⁶-Pro⁷-Phe⁸ motif induced by this electronic control. AII analogues containing electron-deficient aromatic residues at position 6 presented reduced selectivity for the AT2 receptor in contrast to electron-rich aromatic residues. For instance, [4-NO₂-F]⁶-AII displayed 26 times lower AT2R selectivity in comparison to [Y]⁶-AII, but low micromolar affinity for AT1R. Along the same line, [F]⁶-AII presented almost 4 times lower selectivity for AT2R in comparison to the [Y]⁶-AII analogue. This is the first time that a strategy is described to control ligand-receptor subtype selectivity via delicate tuning of aromatic electronics. This strategy could be potentially adapted to other peptidergic GPCR subtypes where the ligand encompasses a proline or an aromatic-proline motif (i.e., see Supplementary Table S7). Indeed, we were intrigued to indirectly validate the strength of this methodology through uncovering a correlation of ligand stereoelectronic control with receptor subtype specificity for the Proteolytically Activated PAR1 and PAR4 receptor subtypes.[29] Although authors of this study had not originally pinpointed the stereoelectronic significance of 4-X-Phe substitution in their strategy to design PAR1/PAR4 selective ligands, they used 4-substituted phenylalanine at position 2 of the GYPGKF native sequence, which carries an electron-rich (-OH), with electron-neutral (-H), and electron-deficient (-F) groups, and produced analogues conferring PAR4 selectivity, no receptor subtype selectivity, and higher PAR1 selectivity, respectively (Supplementary Table S8).

The selective, high affinity, and equipped with discrete conformational plasticity AT2R analogue [Y]⁶-AII (we name it AGT2AG), derived in the frame of this strategy, stimulates the activity of AT2R in PC12W cells and also inhibits MCF-7 breast carcinoma cellular proliferation. *In vivo* experiments are currently underway to test the potential of [Y]⁶-AII as a negative regulator in the growth of breast and pancreatic carcinoma cells through AT2R signaling.

■ METHODS

For methods see Supporting Information.

ASSOCIATED CONTENT

AUTHOR INFORMATION

Corresponding Author

*E-mail: agtzakos@gmail.com.

Present Address

○Biological Crystallography Lab, Department of Biology and Biotechnology, University of Pavia, Italy.

Notes

Patent WO2013/091883A2 regarding the experimental data described here has been filed.

The authors declare no competing financial interest.

ACKNOWLEDGMENTS

REFERENCES

(1) Venkatakrishnan, A. J., Deupi, X., Lebon, G., Tate, C. G., Schertler, G. F., and Babu, M. M. (2013) Molecular signatures of G-protein-coupled receptors. *Nature 494*, 185−194.

(2) Lagerstrom, M. C., and Schioth, H. B. (2008) Structural diversity of G protein-coupled receptors and significance for drug discovery. *Nat. Rev. Drug Discovery 7*, 339−357.

(3) Katritch, V., Kufareva, I., and Abagyan, R. (2011) Structure based prediction of subtype-selectivity for adenosine receptor antagonists. *Neuropharmacology 60*, 108−115.

(4) Tzakos, A. G., Bonvin, A. M., Troganis, A., Cordopatis, P., Amzel, M. L., Gerothanassis, I. P., and van Nuland, N. A. (2003) On the molecular basis of the recognition of angiotensin II (AII). NMR structure of AII in solution compared with the X-ray structure of AII bound to the mAb Fab131. *Eur. J. Biochem. 270*, 849−860.

(5) Tzakos, A. G., Gerothanassis, I. P., and Troganis, A. N. (2004) On the structural basis of the hypertensive properties of angiotensin II: a solved mystery or a controversial issue? *Curr. Top Med. Chem. 4*, 431−444.

(6) de Gasparo, M., Catt, K. J., Inagami, T., Wright, J. W., and Unger, T. (2000) International union of pharmacology. XXIII. The angiotensin II receptors. *Pharmacol. Rev. 52*, 415−472.

(7) Ichiki, T., Labosky, P. A., Shiota, C., Okuyama, S., Imagawa, Y., Fogo, A., Niimura, F., Ichikawa, I., Hogan, B. L., and Inagami, T. (1995) Effects on blood pressure and exploratory behaviour of mice lacking angiotensin II type-2 receptor. *Nature 377*, 748−750.

(8) Doi, C., Egashira, N., Kawabata, A., Maurya, D. K., Ohta, N., Uppalapati, D., Ayuzawa, R., Pickel, L., Isayama, Y., Troyer, D., Takekoshi, S., and Tamura, M. (2010) Angiotensin II type 2 receptor signaling significantly attenuates growth of murine pancreatic carcinoma grafts in syngeneic mice. *BMC Cancer 10*, 67.

(9) Pickel, L., Matsuzuka, T., Doi, C., Ayuzawa, R., Maurya, D. K., Xie, S. X., Berkland, C., and Tamura, M. (2010) Overexpression of angiotensin II type 2 receptor gene induces cell death in lung adenocarcinoma cells. *Cancer Biol. Ther. 9*, 277−285.

(10) Steckelings, U. M., Larhed, M., Hallberg, A., Widdop, R. E., Jones, E. S., Wallinder, C., Namsolleck, P., Dahlof, B., and Unger, T. (2010) Non-peptide AT2-receptor agonists. *Curr. Opin. Pharmacol. 11*, 187−192.

(11) Bosnyak, S., Welungoda, I. K., Hallberg, A., Alterman, M., Widdop, R. E., and Jones, E. S. (2010) Stimulation of angiotensin AT2 receptors by the non-peptide agonist, Compound 21, evokes vasodepressor effects in conscious spontaneously hypertensive rats. *Br. J. Pharmacol. 159*, 709−716.

(12) Widdop, R. E., Jones, E. S., Hannan, R. E., and Gaspari, T. A. (2003) Angiotensin AT2 receptors: cardiovascular hope or hype? *Br. J. Pharmacol. 140*, 809−824.

(13) Ludwig, M., Steinhoff, G., and Li, J. (2012) The regenerative potential of angiotensin AT2 receptor in cardiac repair. *Can. J. Physiol. Pharmacol. 90*, 287−293.

(14) Guimond, M. O., Wallinder, C., Alterman, M., Hallberg, A., and Gallo-Payet, N. (2013) Comparative functional properties of two structurally similar selective nonpeptide drug-like ligands for the angiotensin II type-2 (AT(2)) receptor. Effects on neurite outgrowth in NG108-15 cells. *Eur. J. Pharmacol. 699*, 160−171.

(15) Unal, H., Jagannathan, R., Bhatnagar, A., Tirupula, K., Desnoyer, R., and Karnik, S. S. (2013) Long range effect of mutations on specific conformational changes in the extracellular loop 2 of angiotensin II type 1 receptor. *J. Biol. Chem. 288*, 540−551.

(16) Fillion, D., Cabana, J., Guillemette, G., Leduc, R., Lavigne, P., and Escher, E. (2013) Structure of the human angiotensin II type 1 (AT1) receptor bound to angiotensin II from multiple chemoselective photoprobe contacts reveals a unique peptide binding mode. *J. Biol. Chem. 288*, 8187−8197.

(17) Tuccinardi, T., and Martinelli, A. (2007) Computational approaches on angiotensin receptors and their ligands: recent developments and results. *Curr. Med. Chem. 14*, 3105−3121.

(18) Thomas, K. M., Naduthambi, D., and Zondlo, N. J. (2006) Electronic control of amide cis-trans isomerism via the aromatic-prolyl interaction. *J. Am. Chem. Soc. 128*, 2216−2217.

(19) Granier, S., Manglik, A., Kruse, A. C., Kobilka, T. S., Thian, F. S., Weis, W. I., and Kobilka, B. K. (2012) Structure of the delta-opioid receptor bound to naltrindole. *Nature 485*, 400−404.

(20) Warne, T., Serrano-Vega, M. J., Baker, J. G., Moukhametzianov, R., Edwards, P. C., Henderson, R., Leslie, A. G., Tate, C. G., and Schertler, G. F. (2008) Structure of a beta1-adrenergic G-protein-coupled receptor. *Nature 454*, 486−491.

(21) Zondlo, N. J. (2013) Aromatic-proline interactions: Electronically tunable CH/π interactions. *Acc. Chem. Res. 46*, 1039−1049.

(22) Ballesteros, J. A., and W, H. (1995) Integrated methods for the construction of three dimensional models and computational probing of structure-function relations in G-protein coupled receptors. *Methods Neurosci. 25*, 366−428.

(23) Tamura, M., Wanaka, Y., Landon, E. J., and Inagami, T. (1999) Intracellular sodium modulates the expression of angiotensin II subtype 2 receptor in PC12W cells. *Hypertension 33*, 626−632.

(24) Meffert, S., Stoll, M., Steckelings, U. M., Bottari, S. P., and Unger, T. (1996) The angiotensin II AT2 receptor inhibits proliferation and promotes differentiation in PC12W cells. *Mol. Cell. Endocrinol. 122*, 59−67.

(25) George, A. J., Thomas, W. G., and Hannan, R. D. (2010) The renin-angiotensin system and cancer: old dog, new tricks. *Nat. Rev. Cancer 10*, 745−759.

(26) Nakajima, M., Hutchinson, H. G., Fujinaga, M., Hayashida, W., Morishita, R., Zhang, L., Horiuchi, M., Pratt, R. E., and Dzau, V. J. (1995) The angiotensin II type 2 (AT2) receptor antagonizes the growth effects of the AT1 receptor: gain-of-function study using gene transfer. *Proc. Natl. Acad. Sci. U.S.A. 92*, 10663−10667.

1424

dx.doi.org/10.1021/cb500063y | *ACS Chem. Biol.* 2014, 9, 1420−1425

(27) Li, H., Qi, Y., Li, C., Braseth, L. N., Gao, Y., Shabashvili, A. E., Katovich, M. J., and Sumners, C. (2009) Angiotensin type 2 receptor-mediated apoptosis of human prostate cancer cells. *Mol. Cancer Ther.* 8, 3255−3265.

(28) Muscella, A., Greco, S., Elia, M. G., Storelli, C., and Marsigliante, S. (2002) Angiotensin II stimulation of Na+/K+ATPase activity and cell growth by calcium-independent pathway in MCF-7 breast cancer cells. *J. Endocrinol.* 173, 315−323.

(29) Faruqi, T. R., Weiss, E. J., Shapiro, M. J., Huang, W., and Coughlin, S. R. (2000) Structure-function analysis of protease-activated receptor 4 tethered ligand peptides. Determinants of specificity and utility in assays of receptor function. *J. Biol. Chem.* 275, 19728−19734.

1425

dx.doi.org/10.1021/cb500063y | *ACS Chem. Biol.* 2014, 9, 1420−1425